

# Reaction Graphs for Square Antiprism Rearrangements

J. Brocas

Chimie Organique, Faculté des Sciences, Université Libre de Bruxelles, 50, avenue F. D. Roosevelt,  
B-1050 Bruxelles, Belgium

Received June 17, 1994<sup>®</sup>

We obtain the reaction graphs for the rearrangements of the trans family square antiprisms. The automorphism groups of these graphs are analyzed and expressed as products of well-known permutation groups.

## 1. INTRODUCTION

The  $D_{4d}$  square antiprism is one of the 257 polyhedra having eight vertices.<sup>1</sup> Among these polyhedra, 14 have only triangular faces. These so-called deltahedra have been discussed extensively in previous work. For instance, King<sup>2</sup> has tabulated degenerate diamond-square-diamond (dsd) processes involving these deltahedra. The interest for deltahedra and dsd is justified by the fact that these geometries and dynamic processes are favorable ones.<sup>3</sup>

The square antiprism, in spite of its pair of quadrilateral faces, seems to be at least as stable as deltahedra of chemical interest such as the  $D_{2d}$  dodecahedron,<sup>4–10</sup> the  $D_{6h}$  hexagonal bipyramid,<sup>4,5,8</sup> and the  $D_{3d}$  bicapped trigonal antiprism.<sup>5,8</sup> Hence, much, theoretical work has been devoted to the study of the static and dynamic properties of the square antiprism.

King<sup>11</sup> has pointed out that the square antiprism is one of the octacoordinate polyhedra compatible with  $sp^3d^4$  hybridization. The cube, hexagonal bipyramid,  $D_{2d}$  dodecahedron and the square antiprism are octacoordinate polyhedra whose point group are subgroups of the hyperoctahedral group (vide infra); this gives rise to the hyperoctahedral restriction proposed by the same author<sup>12,13</sup> who has also discussed the possibility of double degenerate dsd processes interconverting  $D_{2d}$  dodecahedra via a  $D_{4d}$  square antiprism intermediate.<sup>2,14</sup>

Modes of rearrangements<sup>15,16</sup> have been used to analyze the dynamics of trans and antipodal families of square antiprisms and the symmetry properties of the paths of steepest descent and transition states of the trans family interconversion have been obtained.<sup>17,18</sup>

While modes of rearrangements reflect the symmetry of the molecular framework in its dynamic aspects, reaction graphs are related to the symmetry of the potential energy surface via the graph isomorphism group. Since the pioneer work of Balaban and co-workers,<sup>19</sup> increasing efforts have been devoted to chemical applications of graph theory and to the derivation of symmetry properties of graphs, including graphs with high degree and order. Details may be found elsewhere (see ref 20 and previous work cited there).

In the present work, we derive the graphs for each of the modes of rearrangements of the trans family of the square antiprism. We obtain also the automorphism group of these graphs. In spite of the relatively small number of vertices and edges, some of these groups are of very high order.

In section 2, we derive some properties of the graphs from the structure of the modes of rearrangements. The automorphism groups of the graphs are discussed in section 3.

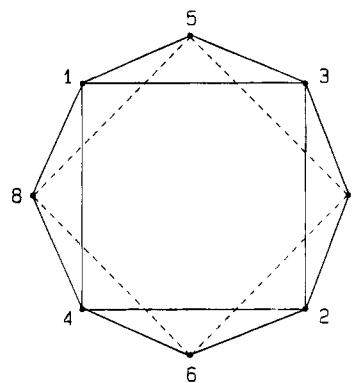


Figure 1. Skeleton labeling of the square antiprism.

## 2. GRAPHS AND MODES OF REARRANGEMENTS

The  $D_{4d}$  square antiprism is represented in Figure 1, as viewed along its  $C_4$  axis. The site labeling of the skeleton is as in ref 17. We consider the trans family used in this previous work: it is the set of configurations where the pairs of ligands {1,2}, {3,4}, {5,6}, {7,8} are trans to each other, i.e., are on the same square face diagonal.

The hyperoctahedral group  $S$  permutes the ligands on the skeleton sites

$$S = L \wedge K \quad (1)$$

$$L = [I, (12)] \otimes [I, (34)] \otimes [I, (56)] \otimes [I, (78)] \quad (2)$$

$$K = [I, (1357)(2468), (1753)(2864), (1375)(2486), (1573)(2684), (1537)(2648), (1735)(2846), (135)(246), (153)(264), (137)(248), (173)(284), (157)(268), (175)(286), (357)(468), (375)(486), (13)(57)(24)(68), (15)(37)(26)(48), (17)(35)(28)(46), (13)(24), (15)(26), (17)(28), (35)(46), (37)(48), (57)(68)] \quad (3)$$

The subgroup  $L$  permutes ligands within the same trans pair;  $K$ , isomorphic to  $S_4$ , permutes the four square face diagonals, hence the actions of both  $L$  and  $K$  preserve the trans relationship, i.e., ligands which are trans to each other remain trans to each other.<sup>12,13,17</sup>

In eqs 1 and 2,  $\wedge$  and  $\otimes$  denote a semidirect and direct product respectively: when two groups have only one common element (the identity  $I$ ), their product is called *direct* when each element of one of them commutes with every element of the other. It is called *semidirect* when one subgroup, as a set, commutes with every element of the other. In the present case,  $L$  commutes with every element of  $K$  (but  $K$  does not commute with every element of  $L$ ).

<sup>®</sup> Abstract published in *Advance ACS Abstracts*, December 1, 1994.

**Table 1.** Modes of Rearrangements

$i$	$y_i$	$\delta_i$	$q_i$
1	I	1	1
2	(13) (24) (78)	1	2
3	(15) (26)	4	24
4	(358467)	4	24
5	(18) (27) (35) (46)	2	4
6	(5768)	2	4
7	(1375)(2486)	4	24
8	(386475)	4	24
9	(135) (246)	8	12
10	(1728)	8	24
11	(13) (24)	4	8
12	(78)	4	8
13	(14) (23) (78)	1	2
14	(12) (34)	1	2

Therefore, the product of K and L is semidirect. On the other hand, all the elements of L commute with each other, and L may therefore be expressed as a direct product (see eq 2). Finally, the product is called *weak direct* when the two groups, as sets, commute with each other.

We also recall the permutational expression of the skeleton point group  $G$ , a subgroup of S and isomorphic to  $D_{4d}$  (see Figure 1):

$$G = A \cup A \sigma \quad (4)$$

$$A = [I, (1324)(5768), (1423)(5867), (12)(34)(56)(78), \\ (15)(26)(38)(47), (17)(28)(35)(46), (16)(25)(37)(48), \\ (18)(27)(36)(45)] \quad (5)$$

$$A \sigma = [(13)(24)(78), (12)(57)(68), (14)(23)(56), \\ (34)(58)(67), (15372648), (18462735), (17452836), \\ (16382547)] \quad (6)$$

where  $\cup$  means union and  $\sigma$  is an improper symmetry operation of the molecular skeleton.

The following results have been obtained previously: The number of configurations of the trans family is<sup>13,17</sup>

$$p = \frac{|S|}{|A|} = \frac{384}{8} = 48 \quad (7)$$

where  $|A|$  means "order of A". The number of modes of rearrangements is<sup>17</sup>

$$z = 14 \quad (8)$$

The mode of rearrangement  $M(y_i)$  is the set of permutations which are indistinguishable from  $y_i$  for symmetry reasons.

The mode generators  $y_i$  ( $i = 1, 2, \dots, 14$ ) are listed in Table 1 where the connectivity  $\delta_i^{21}$  of the modes is also given ( $\delta_i$  is the number of configurations reached in *one step* of a given mode  $i$  from an arbitrary starting configuration). Details about the underlying definitions may be found in Refs 15, 16, and 22.

The last column of Table 1 shows another important information namely the value of  $q_i$  which is the number of configurations reached in an *arbitrary number of steps* of a given mode  $i$ . These values have been obtained previously.<sup>18</sup>

In the present case all the modes are self-inverse,<sup>23</sup> and, therefore, the degree of the corresponding graph is the connectivity  $\delta_i$ .<sup>24</sup> The order of the graph is equal to  $q_i$ .

The  $q_i$  vertices of the graph for mode  $i$  will be labeled by the configuration symbols. Such symbols have been pro-

posed previously<sup>13</sup> and used in ref 18. An alternative more compact convention is as follows: the upper square face is defined as the face bearing ligand 1. When the molecule is seen from above, let a, b, and c be the labels of the three ligands which appear when moving clockwise and starting from 1. The symbol of this configuration is then abc. For instance, the configuration of Figure 1 is 537. It is convenient to replace the ligand labels 4, 6, and 8 by  $\bar{3}$ ,  $\bar{5}$ , and  $\bar{7}$ , respectively. Hence, the symbols consist of the numerals 3, 5, and 7 written in any of the  $3!$  possible orders. Each numeral has eventually an upper bar, this giving rise to  $2^3$  extra possibilities. The total number of symbols is of course  $3! \cdot 2^3 = 48$ . In this convention, configuration enantiomeric to abc is  $\bar{c}\bar{b}\bar{a}$ . The parity rule, established elsewhere,<sup>18,22</sup> is easy to apply with the present convention: the configurations represented by symbols having an even number of bars have the same parity as configuration 537 (say even, e). The others are odd, o. In fact, as seen in eqs 2 and 3, the group K contains only even permutations. Therefore, permutation of the diagonals, which is described by K, does not influence parity. Only permutations on a given diagonal can modify parity, as shown by L. The configuration symbols have another interesting characteristic, namely the order in which the numerals appear. Disregarding the upper bars, we will distinguish the symbols 537, 375, and 753 from 573, 735, and 357. The former are obtained from 537 by even permutation of the numerals 5, 3, and 7 and will be called, arbitrarily, + configurations. The latter, obtained similarly by odd permutations, will be called - configurations. Using both characteristics, (e/o and +/-) it is easy to obtain the list of  $q_i$  configurations reached in an arbitrary number of steps of mode  $i$ .

To do this we notice that the 14 modes of rearrangements consist of seven pairs of enantiomeric modes,<sup>15,17</sup> i.e., {1,2}, {3,4}, {5,6}, {7,8}, {9,10}, {11,12}, {13,14}. The configurations generated from a starting one in one step of a given mode are enantiomeric to those generated by the other mode of the same pair. Moreover, within each pair, one mode is even (i.e., does not change the parity of the configurations), while the other one is odd.<sup>17,22</sup> the modes  $i = 1, 3, 5, 7, 9, 11, 14$  are even. The list of configurations generated by each mode is given in Table 2, where the columns refer to modes and the lines to configurations. The starting configuration is 537 (see Figure 1) for each mode. The heavy horizontal lines delimitate eight boxes. In each box, the upper bars are disposed in the same way indicated by the triplet of + and - signs. For instance, in the last box, the ++- triplet means that the upper bar is on the last numeral of the configuration symbol. The configurations in boxes, 5, 6, 7, and 8 are enantiomeric to those of boxes 1, 2, 3, and 4, respectively, and the configuration of the first line in box 5 is enantiomeric to the one in the first line of box 1, etc. The configurations are alternatively + and - starting with + in the first line of box 1 until the last line of box 4. The first line of box 5 is - and so on alternatively until the last line of box 8. The symbol  $\Delta$  refers to configurations reached from the starting in one step of the mode  $i$ . The symbol O refers to configurations reached after multisteps.

We may now turn our attention to the reaction graphs for the different modes. They are constructed in the usual way: vertices correspond to configurations and edges to interconversions via the considered mode.

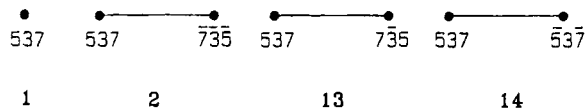


Figure 2. Graphs for modes 2, 13, and 14.

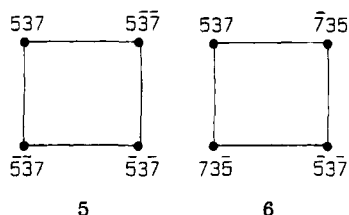


Figure 3. Graphs for modes 5 and 6.

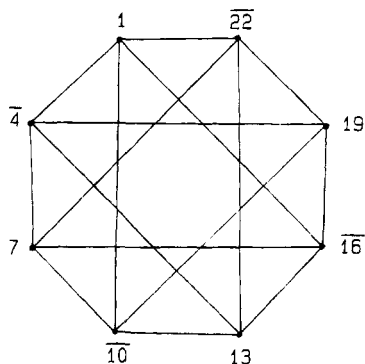


Figure 4. Graph for mode 12.

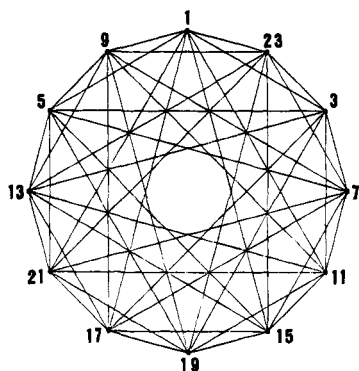


Figure 5. Graph for mode 9.

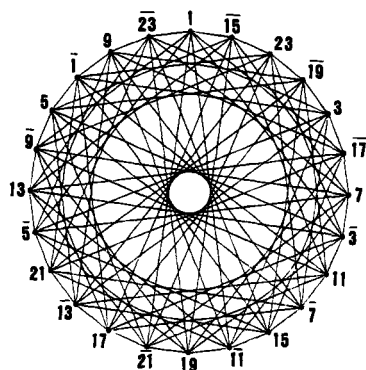


Figure 6. Graph for mode 10.

In Figures 2–8, we represent the graphs for the various modes. Some properties of these graphs may be understood using arguments similar to those of ref 18. Note however that, in this previous work, the improper operations of the molecular point group were even permutations. In this case, enantiomers as well as enantiomeric modes are of the same parity, whereas, in the present case, improper operations are

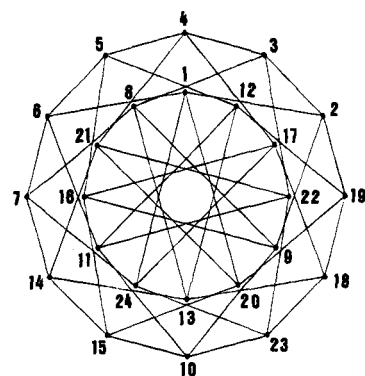


Figure 7. Graph for mode 3.

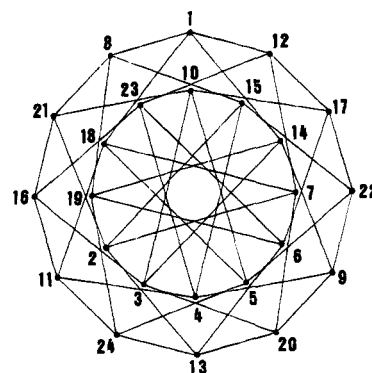


Figure 8. Graph for mode 7.

odd permutations. Hence, enantiomers as well as enantiomeric modes are of different parity.

In the present case, any even mode generates a graph  $g$  whose vertices are even configurations. In such a graph, pairs of enantiomers are excluded. For the enantiomeric mode, the graph  $\tilde{g}$  contains the same number of even and odd configurations. It is bipartite: only edges from even (odd) to odd (even) configuration are possible. For  $\tilde{g}$  there exist two possibilities.

(a) The vertices of  $\tilde{g}$  consist exclusively of pairs of enantiomeric configurations. If  $g$  contains  $u \rightarrow v$  it does not contain  $\bar{u} \rightarrow \bar{v}$  and  $\tilde{g}$  contains  $u \rightarrow \bar{v}$  and  $\bar{u} \rightarrow v$  ( $\bar{u}$  is the configuration enantiomeric to  $u$ ). Hence, the number of vertices of  $\tilde{g}$  is twice that of  $g$ . The pairs of enantiomeric modes  $\{1,2\}$  and  $\{9,10\}$  are of this type (See Table 2, Figures 2, 5, and 6).

(b) The vertices of  $\tilde{g}$  contain no pair of enantiomeric configurations. To any edge  $u \rightarrow v$  in  $g$  corresponds an edge  $u \rightarrow \bar{v}$  in  $\tilde{g}$ . Let  $\tilde{V} = E \cup O$  be the set of vertices of  $\tilde{g}$  ( $E$  and  $O$  are the even and odd vertices in  $\tilde{V}$ ). Then  $V = E \cup \bar{O}$  is the set of vertices of  $g$  ( $\bar{O}$  is the set of vertices enantiomeric to those of  $O$ ). Hence,  $g$  and  $\tilde{g}$  are isomorphic graphs, both bipartite: the graph  $\tilde{g}$  is obtained by replacing the odd configurations of  $g$  by their enantiomer. The graphs for the pairs of modes  $\{3,4\}$  (see Figure 7),  $\{5,6\}$  (see Figure 3),  $\{7,8\}$  (see Figure 8),  $\{11,12\}$  (see Figure 4), and  $\{13,14\}$  (see Figure 2) are of this type.

It might be convenient to dispose of simple rules to describe the effect of the modes on the configuration symbols. We omit the trivial modes 1, 2, 13, and 14 in the subsequent arguments, and we only discuss one mode of each remaining enantiomeric pair, except for the pair  $\{9,10\}$ .

Mode 12, as seen in Figure 4 adds a bar on one of the numerals of the configuration symbols at each step (adding an upper bar to a numeral having an upper bar is merely

**Table 2.** Configurations Reached by Each Mode

		1	2	3	4	5	6	7	8	9	10	11	12	13	14	
1.	537	Δ	○	○	○	○	○	○	○	○	○	○	○	○	○	
2.	573			Δ				○								+
9.	753			○	○			○	○	Δ	○					+
10.	735			○				○				Δ				+
23.	375			○	○			○	○	Δ	○					
24.	357			Δ				○								
19.	537			○	○	Δ		○	○	○	○	○	○			
20.	573			Δ				○								+
15.	753			○	○			○	○	Δ	○					-
16.	735			○				○				Δ				-
17.	375			○	○			○	○	Δ	○					
18.	357			○				Δ								
13.	537			○	○	○	○	○	○	○	○	○	○		Δ	
14.	573			○				Δ								-
21.	753			○	○			○	○	Δ	○					+
4.	735			○				○				Δ				-
5.	375			○	○			○	○	Δ	○					
12.	357			○				Δ								
7.	537			○	○	Δ		○	○	○	○	○	○			
8.	573			○				Δ								-
3.	753			○	○			○	○	Δ	○					-
22.	735			○				○				Δ				+
11.	375			○	○			○	○	Δ	○					
6.	357			Δ				○								
	735			Δ							○					
	375				Δ				○							-
	357										Δ					-
	537				○				○				Δ			-
	573										Δ					
	753				Δ				○							
	735						Δ				○					
	375				Δ				○							-
	357										Δ					+
	537				○				○				Δ			+
	573										Δ					
	753				○				Δ							
	735										○			Δ		
	375				○				Δ							+
	357										Δ					-
	537				○				○				Δ			+
	573										Δ					
	753				○				Δ							
	735						Δ				○					
	375				○				Δ							+
	357										Δ					+
	537				○				○				Δ			-
	573										Δ					
	753				Δ				○							

suppressing the bar). Hence, the order of the numerals is not modified: the eight configurations obtained are 537 with or without upper bars. Mode 5 adds two bars on the two first or last numerals: the four configurations 537 having zero or two bars are generated.

One step of mode 9 amounts to perform a clockwise or a counterclockwise cyclic permutation of the three numerals of the symbol: 537 gives 375 or 753. It moreover either does not modify the obtained symbol or adds two upper bars to it. Hence, it generates the 12 configurations which are even and +. One step of mode 10 permutes the two first or the two last numerals of the symbol and moreover adds 1 or 3 upper bars to it. The 24 configurations which are reached are the 12 even + and the 12 odd - ones.

As it appears clearly from Figures 7 and 8, modes 3 and 7 give rise to isomorphic graphs. To understand this point, let us clarify the effect of these modes on the configuration symbols.

(i) Mode 3 permutes the two initial or the two final numerals of the symbol and adds an upper bar to both of them or to none of them. In this way the initial configuration 537 is transformed into 573,  $\overline{573}$ , 357, and  $\overline{357}$  in one step. Successive applications of this rule generate the 24 even configurations.

(ii) Mode 7 also permutes the two initial or the two final numerals of the symbol and adds an upper bar to one of them and to the numeral which is not permuted. For instance  $\overline{537}$  gives rise to 573,  $\overline{573}$ , 357, and  $\overline{357}$  in one step. Successive applications of this rule also generates the 24 even configurations.

Hence, the relation between a configuration and its "opposite" plays a special role in this isomorphism between modes 3 and 7: we call opposite two configurations which are interconverted by adding a bar to the first and last numeral of the symbol (This is exactly the effect of mode 14, see Figure 2.). We see that the neighbors of a

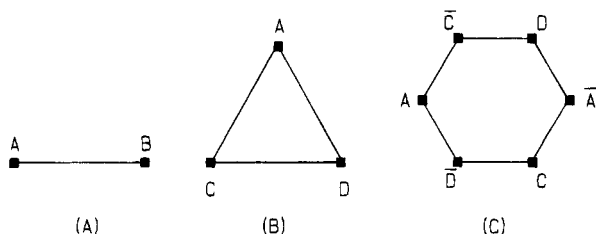


**Figure 9.** Homomorphic mappings of the graphs (a) of Figure 4 (b) Figure 5, and (c) Figure 6.

configuration in the graph for mode 3 are the neighbors of the opposite configuration in the graph of mode 7. This is why these graphs are isomorphic. Opposite configurations in the graph for mode 3 are at opposite positions (i.e., on the same diameter of the inner (outer) circle). The relabeling of vertices underlying the isomorphism is as follows: in graph of mode 3 (Figure 7), first permute the labels of the pairs of vertices which are on the same side of a given diameter, one on the outer circle, one on the inner circle, e.g., 1 and 4, 3 and 12, ... etc and second perform a  $\pi$  rotation of the inner circle. The resulting labeling is that of the graph of mode 7 (Figure 8).

### 3. SYMMETRY OF THE REACTION GRAPHS

The interest for the automorphism groups of reaction graphs has been initiated in a series of papers on "symmetry properties of chemical graphs" by Randić and co-workers. The automorphism group of a graph is the set of permutations of its vertices leaving the set of edges invariant. This group can be established by finding the canonical labeling of the graph. Details about this and other methods and examples may be found in refs 20, 25, 26, and 27 and in previous work cited there.

In the present paper, we use a computer program<sup>28</sup> whose input is the list of the edges between labeled vertices and whose output is the order of the graph automorphism group and the generators of this group, given as permutations of the labeled vertices. The results are given below, where  $\theta_i$  is the automorphism group of the graph generated by mode  $i$ . Note also that the correspondence between the labels of the vertices (1, 2, ..., 24) and the isomer symbols are given in Table 2.

$$\theta_{12} = \{S_4(1,7,13,19) \otimes S_4(\bar{4},\bar{10},\bar{16},\bar{22})\} \wedge [I,(1,\bar{4})(7,\bar{10})(13,\bar{16})(19,\bar{22})] \quad (9)$$

Hence,  $|\theta_{11}| = |\theta_{12}| = (4!)^2 \times 2 = 1152$ , since  $\theta_{11}$  and  $\theta_{12}$  are isomorphic. The structure of  $\theta_{12}$  is obtained from Figure 4 where it appears that the vertices of the graph may be subdivided into two sets  $A = \{1,7,13,19\}$  and  $B = \{\bar{4},\bar{10},\bar{16},\bar{22}\}$  such that each vertex of  $A$  has all the vertices of  $B$  as neighbors and vice versa. The graph  $\theta_{12}$  is isomorphic to  $K_{4,4}$ , the complete bipartite graph of order 8. Such a graph is of course invariant for any permutation within  $A$  or  $B$  (expressed by the product of two symmetric groups of degree 4,  $S_4$ ) and for the permutation of the two sets  $A$  and  $B$  (expressed by the last factor of eq 9). In fact, the graph of Figure 4 may be transformed by homomorphic mapping<sup>26</sup> into the graph of Figure 9(a). In this mapping, the vertices of set  $A$  are replaced by the single vertex  $A$  and similarly for the vertices of set  $B$ .

The graph for mode 9 shown in Figure 5 has 12 vertices and 48 edges. Its complement has  $(12 \cdot 11)/2 - 48 = 18$  edges. It is easy to realize that this complement consists of three complete disconnected graphs of order four whose vertices are within the sets  $A = \{1,7,13,19\}$ ,  $C = \{3,9,15,21\}$ , and  $D = \{5,11,17,23\}$ , respectively. Since the automorphism group of a graph is the same as that of its complement, one obtains

$$\theta_9 = [S_4(1,7,13,19) \otimes S_4(3,9,15,21) \otimes S_4(5,11,17,23)] \wedge S_3 \quad (10)$$

where  $S_3$  expresses the permutations of the three disconnected graphs with sets of vertices  $A$ ,  $C$ , and  $D$

$$S_3 = \{I, (1,3,5)(7,9,11)(13,15,17)(19,21,23), (1,5,3)(7,11,9)(13,17,15)(19,23,21), (1,3)(7,9)(13,15)(19,21), (1,5)(7,11)(13,17)(19,23), (3,5)(9,11)(15,17)(21,23)\} \quad (11)$$

The order of this automorphism group is  $|\theta_9| = (4!)^3 \times 3! = 82\,944$ , but, as seen above, its structure is rather trivial. Again, homomorphic mapping may be used to transform the graph for mode 9 of Figure 5 into the graph (b) of Figure 9.

The graph for mode 10 of Figure 6 is apparently more complicated, but homomorphic mapping is again useful to understand its structure. The 24 vertices of this graph may be partitioned into six sets, such that the vertices of each set are "at right angles" on the graph:  $A = \{1,7,13,19\}$ ,  $C = \{3,9,15,21\}$ , and  $D = \{5,11,17,23\}$  and  $\bar{A}$ ,  $\bar{C}$ , and  $\bar{D}$  consisting of the vertices representing the enantiomers, respectively. It is seen on the graph that the neighbors of any vertex of  $A$  are all the vertices of  $\bar{C}$  and  $\bar{D}$  and so on. The homomorphic mapping of the graph of Figure 6 is shown in Figure 9(c). The automorphism group  $\theta_{10}$  is written as

$$\theta_{10} = \{S_4^A \otimes S_4^C \otimes S_4^D \otimes S_4^{\bar{A}} \otimes S_4^{\bar{C}} \otimes S_4^{\bar{D}}\} \wedge D_6 \quad (12)$$

where  $D_6$  is, as usually, the symbol for the group of proper operations of the regular hexagon (see Figure 9(c)). The permutational expression of  $D_6$  is obtained from the sets  $A$ ,  $\bar{A}$ , etc. We give below such an expression for one element of each class of  $D_6$ :

$$2 C_6 \rightarrow (1,\bar{3},5,\bar{1},3,\bar{5})(7,\bar{9},11,\bar{7},9,\bar{11}) \times (13,\bar{15},17,\bar{13},15,\bar{17})(19,\bar{21},23,\bar{19},21,\bar{23})$$

$$2 C_3 \rightarrow (1,3,5)(\bar{1},\bar{3},\bar{5})(7,9,11)(\bar{7},\bar{9},\bar{11})(13,15,17) \times (\bar{13},\bar{15},\bar{17})(19,21,23)(\bar{19},\bar{21},\bar{23})$$

$$C_2 \rightarrow (1,\bar{1})(3,\bar{3})(5,\bar{5})(7,\bar{7})(9,\bar{9})(11,\bar{11})(13,\bar{13})(15,\bar{15}) \times (17,\bar{17})(19,\bar{19})(21,\bar{21})(23,\bar{23})$$

$$3 C'_2 \rightarrow (3,5)(\bar{3},\bar{5})(9,11)(\bar{9},\bar{11})(15,17)(\bar{15},\bar{17}) \times (21,23)(\bar{21},\bar{23})$$

$$3 C''_2 \rightarrow (1,\bar{1})(3,\bar{5})(\bar{3},5)(7,\bar{7})(9,\bar{11})(\bar{9},11)(13,\bar{13}) \times (15,\bar{17})(\bar{15},17)(19,\bar{19})(21,\bar{23})(\bar{21},23)$$

The order of  $\theta_{10}$  is  $|\theta_{10}| = (4!)^6 \times 12 = 2\,293\,235\,712$  which looks enormous but is much smaller than  $24! \sim 6 \times 10^{23}$  ...!

**Table 3.** Structure of the Group  $\theta_3$ 

cycle structure	no. of classes	no. of elements in the classes
$1^{24}$	1	1
$1^{16}2^4$	1	6
$1^{12}2^6$	1	6
$1^{82}8$	3	3 + 6 + 6
$1^{42}10$	3	6 + 12 + 24
$2^{12}$	9	1 + 2 + 3 + 6 + 6 + 8 + 12 + 12 + 24
$1^{42}4^3$	1	48
$1^{42}2^4$	1	24
$1^{22}3^4$	5	24 + 24 + 24 + 24 + 24
$1^{22}4^5$	1	48
$3^8$	1	32
$4^6$	10	8 + 12 + 12 + 24 + 24 + 24 + 24 + 32 + 64 + 64
$12^2$	1	64

**Table 4.** Invariant Subgroups of  $\theta_3$ 

order	no. of invariant subgroups	order	no. of invariant subgroups
2	1	64	3
4	2	96	3
8	1	128	1
16	4	192	7
32	2	384	7
48	1		

We were not able to discuss the automorphism group  $\theta_3$  in terms of homomorphic mapping. The following discussion hopefully provides some insight into its structure. Its order is  $|\theta_3| = 768$ , and it may be defined by four generators:

$$t_1 = (4,22)(5,11)(10,16)(17,23)$$

$$t_2 = (5,17)(6,24)(11,23)(12,18)$$

$$t_3 = (2,6)(3,5)(7,19)(8,12)(9,11)(14,18)(15,23) \times (16,22)(17,21)(20,24)$$

$$t_4 = (1,2,3,4,5,6)(7,20,9,22,17,12)(8,21,16,11,24,19) \times (10,23,18,13,14,15) \quad (13)$$

Its 38 conjugacy classes are shown in Table 3 where the number of classes for each cycle structure is given. The last column shows the number of elements in these classes.

By far the most interesting information about  $\theta_3$  is to express it as a product of smaller groups whose properties are known. This can be tried by using the invariant (or normal) subgroups of  $\theta_3$ . There exist 32 such subgroups. Their order is given in Table 4. It is tempting to express  $\theta_3$  as a weak direct product of two (or more) of its invariant subgroups.<sup>29</sup> This requires that the intersection of a pair of subgroups whose product of orders is 768 reduces to the identity element. Unfortunately, such pairs do not exist among the invariant subgroups of  $\theta_3$ .

Another possibility is to use the apparent symmetry of the graph of Figure 7, i.e.,  $D_{12}$ , the group of proper operations of the regular dodecagon (note that it is impossible to find apparent symmetries with rotation axes of order higher than 12, as shown in Table 3 by the order of the elements of  $\theta_3$ ).

As seen from Table 4,  $D_{12}$ , a group of order 24, cannot be an invariant subgroup of  $\theta_3$ . The 24 operations of  $D_{12}$  are readily obtained as permutations of the vertices of the graph of Figure 7. The result is summarized in Table 5.

**Table 5.** Structure of the Group  $D_{12}$ 

class of $D_{12}$	cycle structure	no. of operations
I	$1^{24}$	1
$C_{12}^1, C_{12}^{11}$	$12^2$	2
$C_{12}^5, C_{12}^7$	$12^2$	2
$C_6^1, C_6^5$	$6^4$	2
$C_4^1, C_4^3$	$4^6$	2
$C_3^1, C_3^2$	$3^8$	2
$C_2$	$2^{12}$	1
$6 C_2'$	$2^{12}$	6
$6 C_2$	$1^{42}10$	6

Hopefully, it will be possible to express  $\theta_3$  as a semidirect product  $T \wedge D_{12}$  where  $T$  is one of the two invariant subgroups of  $\theta_3$  which are of order 32 (see Table 4). This new trial also fails! The next convenient solution is then to test if one can find two invariant subgroups of, say  $T'$  and  $T''$  such that  $T' \wedge D_{12} = T''$  and that  $|T'| < 32$ . It appears that one of the four invariant subgroups of  $\theta_3$  which are of order 16 satisfy this requirement. In fact  $T'$  is the only commutative group of order 16.<sup>30</sup> It has only elements of order 2, except the identity itself, and is the direct product of four groups of order 2.

$$T' = [I, \alpha] \otimes [I, \beta] \otimes [I, \chi] \otimes [I, \delta] \quad (14)$$

$$\begin{aligned} \alpha &= cdef & \chi &= a'd'e'f' \\ \beta &= abcd & \delta &= b'c'd'e' \end{aligned} \quad (15)$$

$$\begin{aligned} a &= (1,7)(13,19) & a' &= (1,19)(7,13) \\ b &= (2,8)(14,20) & b' &= (2,20)(8,14) \\ c &= (3,9)(15,21) & c' &= (3,21)(9,15) \\ d &= (4,16)(10,22) & d' &= (4,22)(10,16) \\ e &= (5,17)(11,23) & e' &= (5,11)(17,23) \\ f &= (6,24)(12,18) & f' &= (6,12)(18,24) \end{aligned} \quad (16)$$

The group  $T''$  is of order  $|T''| = 16 \times 24 = 384$ . Some of its properties are discussed in the Appendix.

Finally we arrive at the factorization of  $\theta_3$  as a semidirect product of two groups, one of which is itself a semidirect product:

$$\theta_3 = \{T' \wedge D_{12}\} \wedge [I, \theta] \quad (17)$$

where  $\theta$  is any element of order 2 in  $\theta_3$  not belonging to  $T''$ , e.g.

$$\theta = (4,22)(5,11)(10,16)(17,23) \quad (18)$$

#### 4. CONCLUSIONS

In the present work, we have obtained the reaction graphs for each of the 14 modes of rearrangements interconverting the 48 square antiprism configurations of the trans family.

We have also derived the automorphism groups of these graphs, and we factorized them into products of smaller and more familiar point groups or permutation groups. One of these groups, is of rather enormous order ( $> 2.10^9$ ) but has a quite simple structure. Another one has only 768 elements but is more difficult to visualize.

The model used here is of course a simplified description of the square antiprism interconversions, and the present

Table 6. Structure of the Group T''

cycle structure	no. of classes	no. of elements
1 <sup>24</sup>	1	1
1 <sup>12</sup> 2 <sup>6</sup>	1	6
1 <sup>8</sup> 2 <sup>8</sup>	2	3 + 6
1 <sup>4</sup> 2 <sup>10</sup>	2	6 + 24
2 <sup>12</sup>	4	1 + 3 + 6 + 24
1 <sup>2</sup> 2 <sup>14</sup> 5	2	24 + 24
2 <sup>4</sup> 4 <sup>4</sup>	3	24 + 24 + 24
3 <sup>8</sup>	1	32
4 <sup>6</sup>	3	8 + 24 + 24
6 <sup>4</sup>	1	32
12 <sup>2</sup>	2	32 + 32

results should be compared to the experimental investigations. Recent work in this field<sup>31-36</sup> reports observations of various geometries, among which square antiprism has been described for IF<sub>8</sub><sup>-</sup> and TeF<sub>8</sub><sup>2-</sup>,<sup>35</sup> but it is expected that information about square antiprism interconversions are best obtained from substituted molecular framework rather than from the above ML<sub>8</sub> compounds.

### 5. APPENDIX

The automorphism group of the graph for mode 3 is given by eqs 14-18 and Table 5. The group T'' is an invariant subgroup of  $\theta_3$ . It is of order 384. It has 22 conjugacy classes whose cycle structure and number of elements are given in Table 6. Hence, it is not isomorphic to S given in eq 1 which has 20 conjugacy classes<sup>17</sup> instead of 22.

### ACKNOWLEDGMENT

We thank M. Dehon and J. Liévin for their help in the access to the Symbolic Calculator, R. Vandeloise, for the computer assisted drawing of the graphs, and V. Garin for her patient and careful typing of the text.

### REFERENCES AND NOTES

- (1) Britton, D.; Dunitz, J. D. *Acta Crystallogr.* **1973**, 29A, 362.
- (2) King, R. B. *Inorg. Chem.* **1986**, 25, 506.
- (3) Lipscomb, W. N. *Science* **1966**, 153, 373.
- (4) Hoard, J. L.; Silverton, J. V. *Inorg. Chem.* **1963**, 2, 235.
- (5) Muetterties, E. L.; Wright, C. M. *Quart. Revs* **1967**, 21, 109.
- (6) Muetterties, E. L. *Tetrahedron* **1974**, 30, 1595.
- (7) Muetterties, E. L.; Guggenberger, L. J. *J. Am. Chem. Soc.* **1974**, 96, 1748.

- (8) Burdett, J. K.; Hoffmann, R.; Fay, R. C. *Inorg. Chem.* **1978**, 17, 2553.
- (9) Kepert, D. L. *Inorganic Stereochemistry* (Inorganic Stereochemistry Concepts, Vol. 6) Springer Verlag: 1982.
- (10) Clare, B. W.; Favas, M. C.; Kepert, D. L.; May, A. S. In *Advances in Dynamic Stereochemistry*; Gielen, M., Ed.; Freund Publishing House Ltd.: 1985; p 1.
- (11) King, R. B. *J. Am. Chem. Soc.* **1969**, 91, 7211; Eyring, H.; Walter, J.; Kimball, G. E. *Quantum Chemistry*; Wiley and Sons: New York, 1944. Randić, M. *J. Chem. Phys.* **1962**, 36, 1094. Randić, M. *Croat. Chem. Acta* **1960**, 32, 145.
- (12) King, R. B. *Inorg. Chem.* **1981**, 20, 363.
- (13) King, R. B. *Theor. Chim. Acta* **1981**, 59, 25.
- (14) King, R. B. *Inorg. Chim. Acta* **1981**, 49, 237.
- (15) Hässelbarth, W.; Ruch, E. *Theor. Chim. Acta* **1973**, 29, 259.
- (16) Klemperer, W. G. *J. Am. Chem. Soc.* **1972**, 94, 8360.
- (17) Brocas, J. In *Advances in Dynamic Stereochemistry*; Gielen, M., Ed.; Freund Publishing House Ltd.: 1985; p 43.
- (18) Brocas, J. In *Graph Theory and Topology in Chemistry*; King, R. B., Rouvray, D. H., Eds.; Studies in Physical and Theoretical Chemistry, Elsevier: Amsterdam, 1987; Vol. 51, p 239.
- (19) Balaban, A. T.; Fărcașiu, D.; Bănică, R. *Rev. Roum. Chimie* **1966**, 11, 1205.
- (20) Randić, M.; Klein, D. J.; Katović, V.; Oakland, D. O.; Seitz, W. A.; Balaban, A. T. In *Graph Theory and Topology in Chemistry*, King, R. B., Rouvray, D. H., Eds.; Studies in Physical and Theoretical Chemistry, Elsevier: Amsterdam, 1987; Vol. 51, p 266.
- (21) Muetterties, E. L. *J. Am. Chem. Soc.* **1969**, 91, 1636, 4115.
- (22) Brocas, J.; Gielen, M.; Willem, R. *The Permutational Approach to Dynamic Stereochemistry* McGraw-Hill: New York, 1983.
- (23) Nourse, J. G. *J. Am. Chem. Soc.* **1980**, 102, 4883.
- (24) Balaban, A. T.; Brocas, J. *J. Mol. Struct. (Theochem)* **1989**, 185, 139.
- (25) Randić, M.; Katović, V. *Int. J. Quantum Chemistry* **1982**, 21, 647.
- (26) Randić, M.; Katović, V.; Trinajstić, N. In *Symmetry and Properties of Non-Rigid Molecules*; Maruani, J., Serre, J., Eds.; Studies in Physical and Theoretical Chemistry, Elsevier: Amsterdam, 1983; Vol. 23, p 399.
- (27) Randić, M. *Theor. Chim. Acta* **1985**, 67, 137.
- (28) Cannon, J.; Bosma, W. *Cayley*, Computer Algebra; University of Sidney: Sidney, Australia, 1991.
- (29) Flurry, R. L. In *Symmetry and Properties of Non-Rigid Molecules*; Maruani, J., Serre, J.; Studies in Physical and Theoretical Chemistry, Elsevier: Amsterdam, 1983; Vol. 23, p 113.
- (30) Higman, B. *Applied Group Theoretic and Matrix Methods*; Dover, New York, 1964.
- (31) Suyarov, D. K.; Sh'kolnikova, L. M.; Porai-Koshits, M. A.; Fundamentski, V. S.; Davidovich, R. L. *Doklady Akad. Nauk* **1990**, 331, 1397.
- (32) Aime, S.; Botta, M. *Inorg. Chim. Acta* **1990**, 177, 101.
- (33) Leeaphon, M.; Fanwick, P. E.; Walton, R. A. *J. Am. Chem. Soc.* **1991**, 113, 1424. Leeaphon, M.; Fanwick, P. E.; Walton, R. A. *Inorg. Chem.* **1991**, 30, 4986.
- (34) Luo, X. L.; Michos, D.; Crabtree, R. H. *Inorg. Chem.* **1991**, 30, 4286.
- (35) Christe, K. O.; Sanders, J. C. P.; Schrobilgen, G. H.; Wilson, W. W. *J. Chem. Soc., Chem. Commun.* **1991**, 837.
- (36) Ellis, J. E.; Chi, K. M.; Di Maio, L.; Haggerty, B. S. *Angew. Chem. Int. Ed. Engl.* **1991**, 30, 194.

CI940074S